Performance Improvement of Remote Microphone-Based Virtual Sensing Method for Feedforward Active Noise Control System with Coherence-Adjusting Filter

Tianyu Xie*, Shota Toyooka*, Kenta Iwai†
and Yoshinobu Kajikawa‡
*‡Faculty of Engineering Science, Kansai University, Japan
†College of Information Science and Engineering, Ritsumeikan University, Japan

***Abstract*—In this paper, we propose a new Remote Microphone-based Virtual Sensing (RMVS) method for feedforward active noise control (ANC) system with two coherence adjusting filters (CAF). The feedforward ANC system with RMVS has a poor noise reduction performance under low coherence conditions between signals obtained at reference microphone, error microphone and virtual microphone. The CAF can improve the coherences between the signals obtained at three microphones and prevents the degradation of noise reduction. Unlike the basic feedforward ANC system, the feedforward ANC system with RMVS has three microphone; reference microphone, error microphone and virtual microphone. The low coherence in the combinations of the three microphones yields the degradation of noise reduction performance of the feedforward ANC system with RMVS. Hence, the proposed system utilizes two CAFs in order to improve the performance of the feedforward ANC system with RMVS. One of them adjusts the coherence between the error signal and the estimated desired signal, and another CAF adjusts the coherence between the reference signal and the estimated desired signal. Simulations show that the proposed method improves noise reduction by 10 dB in the frequency band around 1200 Hz where the conventional method degrades the noise reduction, and improves the overall noise reduction by approximately 4 dB.**

I. Introduction

Active noise control (ANC) system[1]-[3] is a solution for the noise problems. Based on the superposition of the sound wave, the ANC system reduces unwanted noise by generating an anti noise that has the same amplitude and the opposite phase of the unwanted noise. The ANC system is classified into two control structures, i.e. feedforward and feedback control structures. In this paper, we focus on the feedfoeward structure to reduce the broadband noise. The basic feedforward ANC system is shown in Fig. 1, where the reference signal picked up by the reference microphone is processed by the ANC controller to generate the anti noise emitted from the secondary loudspeaker. The error microphone is placed at a desired location where noise reduction is realized.

One problem with the feedforward ANC system is that error microphones are not always placed at the desired location. If the error microphone cannot be placed at the desired location, noise reduction may not be obtained. This is due to the limitation of the size of the zone of quiet (ZoQ)[4][5] generated around the error microphone. To solve such problems, virtual sensing technology[6]-[8] is used in ANC systems.

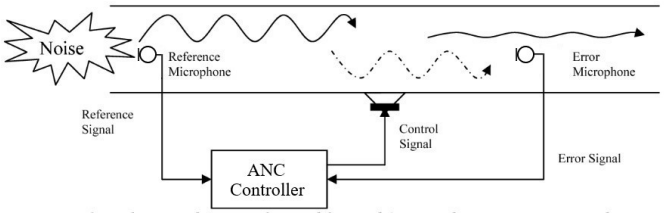

Fig. 1. Structure of basic feedforward ANC system.

There are two methods in virtual sensing techniques, i.e. Remote Microphone-based Virtual Sensing (RMVS)[9] method and Auxiliary Filter-based Virtual Sensing (AFVS)[10] method. In order to achieve noise reduction at the desired location (called the virtual microphone), both methods need to estimate a filter at a tuning stage, and then use this filter in a control stage to realize the noise reduction at the desired location. In this paper, we focus on coherence problems of RMVS method for feedforward ANC system. In RMVS method, the low coherence condition between error microphone and virtual microphone will cause noise reduction performance degrade dramatically. For low coherence condition, the coherence adjusting filter (CAF)[11] can improve the coherence between the signals obtained at each microphone.

In this paper, we use two CAFs to improve the performance of the feedforward ANC system with RMVS. In the proposed system, the first CAF at the tuning stage adjusts the coherence between the error microphone and the virtual microphone, and the second CAF at the control stage adjusts the coherence between the reference microphone and the virtual microphone to improve the performance of noise reduction. Computer simulations are conducted to evaluate the capability of this system to increase the coherences between signals and the reduction of unwanted noise.

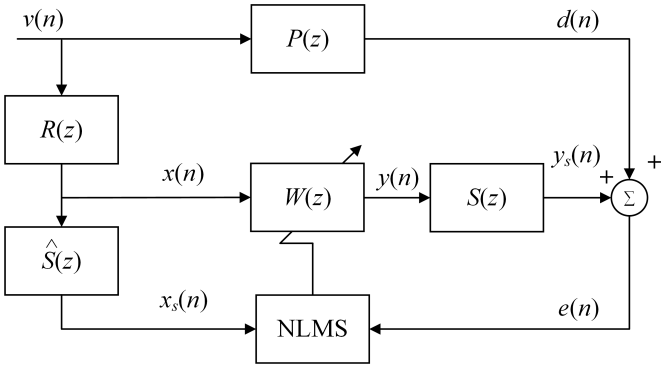

Fig. 2. Block diagram of basic feedforward ANC system.

II. Related work

A. Feedforward ANC system

The block diagram of the basic feedforward ANC system is shown in Fig. 2, where $R(z)$, $P(z)$, and $S(z)$ represent the reference path from the noise source to the reference microphone, the primary path from the noise source to the error microphone, and the secondary path from the secondary loudspeaker to the error microphone, respectively. $\hat{S}(z)$ is the estimated model of the secondary path $S(z)$. The input signal $v(n)$ is unwanted noise. The desired signal $d(n)$ obtained at the error microphone is reduced by the anti noise $y_s(n)$. The anti noise $y_s(n)$ is generated using the noise control filter $W_o(z)$ and the reference signal $x(n)$; $W_o(z)$ is updated using the filtered reference signal $x_s(n)$ and the error signal $e(n)$. The z transform of the error signal $e(n)$ is given by

$$E(z) = D(z) + S(z)W_o(z)X(z). \tag{1}$$

In the case that $E(z) = 0$, the optimal noise control filter $W_o(z)$ is obtained as

$$W_o(z) = \frac{P(z)}{R(z)S(z)}. \tag{2}$$

The performance of the feedforward ANC system can be determined by frequency-domain analysis of the residual error signal $e(n)$. The power spectral density of $e(n)$ is given by

$$S_{ee,\min}(w) = \mathbf{E}[E^*(w)E(w)] = S_{dd}(w) - \frac{S_{dx}^2(w)}{S_{xx}(w)}, \tag{3}$$

where $\mathbf{E}[\cdot]$ is the expectation operator, $E(w)$ is the frequency spectrum of $e(n)$, $S_{dx}(w)$ is the cross power spectral density of $d(n)$ and $x(n)$, $S_{dd}(w)$ is the power spectral density of $d(n)$ and $S_{xx}(w)$ is the power spectral density of $x(n)$, respectively. From (3), the normalized version of $S_{ee,\min}(w)$ can be obtained as

$$S_{ee,\min}(w) = S_{dd}(w)[1 - C_{dx}(w)], \tag{4}$$

$$C_{dx}(w) = \frac{S_{dx}^2(w)}{S_{dd}(w)S_{xx}(w)}, \tag{5}$$

where $C_{dx}(w)$ is the magnitude-squared coherence (MSC) function between unwanted noise $d(n)$ and reference signal $x(n)$. From (4), the error signal $S_{ee,\min}(w)$ is minimized when $C_{dx} = 1$. Hence, the performance of the baisc feedforward ANC system depends on the coherence between signals obtained at the reference and error microphones.

B. Remote Microphone-based Virtual Sensing method

Fig. 3 shows the block diagram of the feedforward ANC system using the RMVS method. $P_m(z)$ and $P_v(z)$ are the impulse responses of the primary paths from the noise source to the error microphone and the virtual microphone, respectively. $S_m(z)$ and $S_v(z)$ are the impulse responses of the secondary paths from the secondary source to the error microphone and the virtual microphone, respectively. RMVS method firstly estimates the transfer function of ratio of $P_v(z)$ to $P_m(z)$ called $C_p(z)$ at the tuning stage as shown in Fig. 3 (a). Subsequently, at the control stage as shown in Fig. 3 (b), this system estimates the desired noise signal at the desired location by using $C_p(z)$.

In the tuning stage, the z transform of the error signal $e_p(n)$ is represented by

$$E_p(z) = D_v(z) - C_p(z)D_m(z). \tag{6}$$

In the case that $E_p(z) = 0$, the $C_p(z)$ is derived as

$$C_p(z) = \frac{P_v(z)}{P_m(z)}. \tag{7}$$

In the control stage, the z transform of error signal $\hat{e}_v(n)$ is written as

$$\hat{E}_v(z) = C_p(z)\hat{D}_m(z) + \hat{S}_v(z)W_R(z)X(z). \tag{8}$$

Then, the optimal noise control filter $W_R(z)$ is obtained in the case that $\hat{E}_v(z) = 0$ as

$$W_R(z) = -\frac{C_p(z)P_m(z)}{R(z)\hat{S}_v(z)} = -\frac{P_v(z)}{R(z)S_v(z)}. \tag{9}$$

In addition, the causality[12] of the $C_p(z)$ must be satisfied. Hence, the error microphone must be located closer to the noise source than the virtual microphone. If the unwanted noise arrived at the virtual microphone location ahead of the error microphone location, the $C_p(z)$ has non-causality and the noise reduction performance is consequently degraded.

Moreover, the performance of the feedforward ANC system with RMVS is related to the coherences between the signals obtained at each microphone. There are many reasons for low correlation conditions, such as reverberation and reflection of sound, distance and obstacles between microphones. The low coherence conditions between reference microphone and virtual microphone, and error microphone and virtual microphone, will degrade the performance of the feedforward ANC system with RMVS. In particular, the performance of noise reduction declines dramatically at the frequency where the coherence degrades.

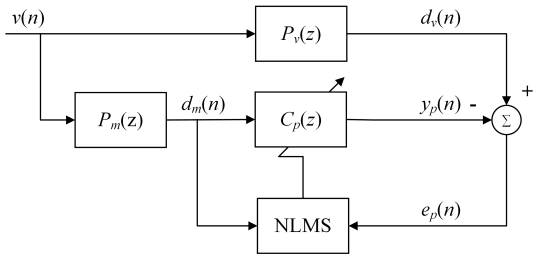

(a) Tuning stage

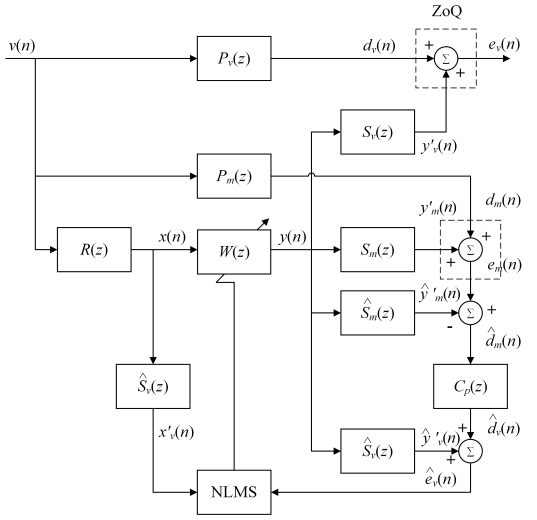

(b) Control stage

Fig. 3. Block diagram of feedforward ANC system with RMVS.

C. Feedforward ANC system with CAF

As discussed in Section II-A and Section II-B, the noise reduction performance of the feedforward ANC system depends on the coherence between signals obtained at each microphone. For the low coherence condition, the coherence-adjusting filter (CAF) can improve the coherence between the signals obtained at each microphone. Fig. 4 shows the block diagram of the basic Feedforward ANC system with CAF. From Fig. 4, this configuration utilizes the CAF $H(z)$ to adjust the coherence between reference signal $x(n)$ and desired signal $d(n)$. The highest coherence condition $x(n-n_d) = d(n)$ cannot be realized, however, an approximate condition $x(n-n_d) \approx d(n)$ can be realized by using the CAF. The output of the CAF in the z transform domain is represented by

$$X_A(z) = H(z)X(z), \tag{10}$$

where $X_A(z)$ is the z transform of the output of the CAF $x_A(n)$, $H(z)$ is the frequency response of the CAF, and $X(z)$ is the z transform of reference signal $x(n)$. When the coherence is completely adjusted, the output of the CAF is $X_A(z) = D(z)/z^{-n_d}$, where z^{-n_d} is delay operator used to update the CAF $H(z)$, and the value of n_d is the sample lag between the initial peaks in the impulse responses of paths

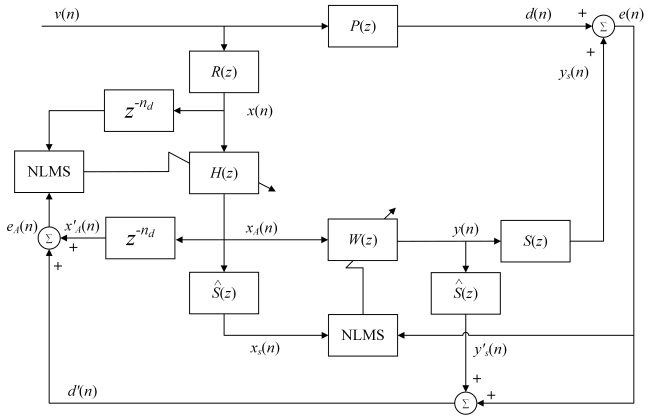

Fig. 4. Block diagram of basic feedforward ANC system with CAF.

$R(z)$ and $P(z)$. Under this condition, the optimal frequency response of CAF should be

$$H(z) = \frac{X_A(z)}{X(z)} = \frac{P(z)}{R(z)z^{-n_d}}. \tag{11}$$

The z transform of the error signal $e(n)$ is given by

$$E(z) = D(z) + S(z)W_C(z)H(z)X(z). \tag{12}$$

In the case that $E(z) = 0$, the optimal noise control filter $W_C(z)$ is obtained as

$$W_C(z) = \frac{P(z)}{S(z)H(z)R(z)} = \frac{z^{-n_d}}{S(z)}. \tag{13}$$

Note that $S(z)$ is a nonminimum phase system. Hence, in order to ensure the causality, the following condition should be satisfied:

$$-n_d + n_s < 0. \tag{14}$$

The additional delay n_d should be

$$n_d > n_s, \tag{15}$$

where n_s is the maximum time delay of the secondary path $S(z)$. More simply, (15) means that the distance between reference microphone and error microphone must greater than the distance between secondary source and error microphone.

CAF $H(z)$ is updated by the adaptive filtering algorithm (e.g., normalized least-mean-square (NLMS) algorithm) represented as

$$\mathbf{h}(n+1) = \mathbf{h}(n) - \frac{\alpha_A e_A(n)\mathbf{x}(n-n_d)}{\|\mathbf{x}(n-n_d)\|^2 + \beta_A}, \tag{16}$$

$$e_A(n) = d'(n) + x'_A(n), \tag{17}$$

where $\mathbf{h}(n)$ is the filter coefficient vector of the CAF, $\mathbf{x}(n)$ is the reference signal vector, α_A is the step size parameter ($0 < \alpha_A < 2$), and β_A is the regularization parameter with a small positive value.

The optimal noise control filter $W_C(z)$ is also updated by NLMS algorithm represented as

$$\mathbf{w}(n+1) = \mathbf{w}(n) - \frac{\alpha e(n)\mathbf{x_s}(n)}{\|\mathbf{x_s}(n)\|^2 + \beta}, \tag{18}$$

where $\mathbf{w}(n)$ is the coefficient vector of the noise control filter $W_C(z)$, $\mathbf{x_s}(n)$ is the filtered reference signal vector, α is the step size parameter ($0 < \alpha < 2$), and β is the regularization parameter with a small positive value, respectively.

III. Proposed System

As discussed in Section II-A, the noise reduction performance of the feedforward ANC system depends on the coherence between the reference signal and desired signal. The RMVS problem of degraded coherence between the error microphone and the virtual microphone shown in Section II-B can be solved using CAF. In this section, the proposed system aims to improve the noise reduction performance of RMVS method by using CAFs at the tuning stage and the control stage, respectively.

From Fig. 5 (a), the proposed system uses the CAF $H_1(z)$ at the tuning stage to adjust $d_m(n)$ to be close to $d_v(n)$. Under the condition of $d_m(n-n_d) \approx d_v(n)$, the output of $H_1(z)$ in the z transform domain becomes $D_{mA}(z) = D_v(z)/z^{-n_d}$, where z^{-n_d} is delay operator used to update the CAF $H_1(z)$, and the value of n_d is the sample lag between the initial peaks in the impulse responses of paths $P_m(z)$ and $P_v(z)$. Under this condition, the optimal CAF $H_1(z)$ should be

$$H_1(z) = \frac{D_{mA}(z)}{D_m(z)} = \frac{P_v(z)}{P_m(z)z^{-n_d}}. \tag{19}$$

The z transform of the error signal $e_p(n)$ in the tuning stage is given by

$$E_p(z) = D_v(z) + C_p(z)H_1(z)D_{mA}(z). \tag{20}$$

$C_p(z)$ is obtained in the case that $E_p(z) = 0$ as

$$C_p(z) = \frac{P_v(z)}{H_1(z)P_m(z)} = z^{-n_d}. \tag{21}$$

In the control stage, from Fig. 5 (b), the proposed system utilizes the CAF $H_2(z)$ to adjust $x(n)$ to be close to $\hat{d}_v(n)$. Under the condition of $r(n-n_r) \approx \hat{d}_v(n)$, the output of $H_2(z)$ in the z transform domain becomes $X_A(z) = \hat{D}_v(z)/z^{-n_r}$, and the value of n_r is the sample lag between the initial peaks in the impulse responses of paths $R(z)$ and $P_v(z)$. Under this condition, the optimal CAF $H_2(z)$ should be

$$\begin{aligned} H_2(z) &= \frac{\hat{D}_v(z)}{X(z)z^{-n_r}} = \frac{C_p(z)H_1(z)P_m(z)}{R(z)z^{-n_r}} \\ &= \frac{P_v(z)}{R(z)z^{-n_r}}. \end{aligned} \tag{22}$$

The z transform of the error signal $\hat{e}_v(n)$ is represented by

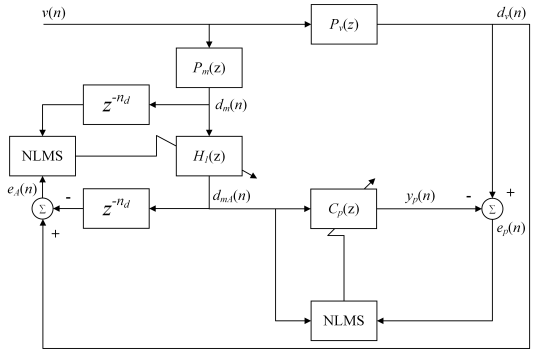

(a) Tuning stage

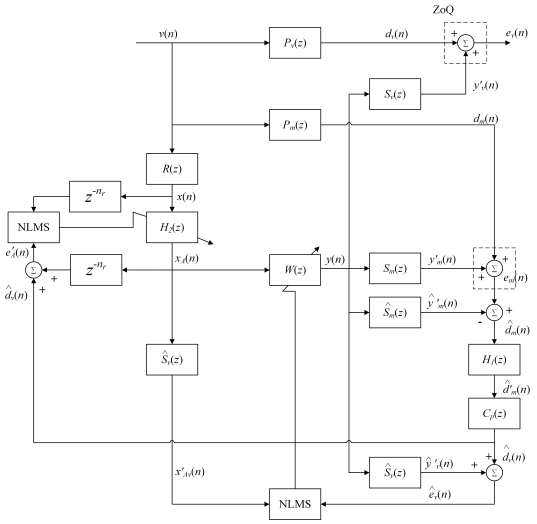

(b) Control stage

Fig. 5. Block diagram of proposed feedforward ANC system with RMVS and CAF.

$$\hat{E}_v(z) = C_p(z)H_1(z)\hat{D}_m(z) + \hat{S}_v(z)W(z)H_2(z)X(z). \tag{23}$$

Then, the noise control filter $W(z)$ is obtained in the case that $\hat{E}_v(z) = 0$ as

$$W(z) = -\frac{C_p(z)H_1(z)P_m(z)}{S_v(z)H_2(z)R(z)} = -\frac{z^{-n_r}}{S_v(z)}. \tag{24}$$

To satisfy the causality of $W(z)$,

$$-n_r + n_{sv} < 0. \tag{25}$$

The additional delay n_r should be

$$n_r > n_{sv}, \tag{26}$$

where n_r is the delay of CAF $H_2(z)$ and n_{sv} is the maximum time delay of the secondary path $S_v(z)$.

IV. Simulation Results

The computer simulations are conducted to demonstrate the increase in the coherences between the signals and the improvement of the noise reduction performance of the proposed

TABLE I
SIMULATION CONDITIONS.

Unwanted noise	White noise
Sampling frequency	8000 Hz
Frequency range	200-2000 Hz
Tap length of primary paths P_m and P_v	300
Tap length of reference path R	200
Tap length of secondary paths S_v and S_m	300
Tap length of noise control filter W	400
Tap length of CAFs H_1 and H_2	400
Step size parameters α and α_A	0.1
Regularization parameters β and β_A	1.0×10^{-6}
Time	37.5 s
Delay n_d	5
Delay n_r	25

Fig. 6. Actual measurement setup in a soundproof room.

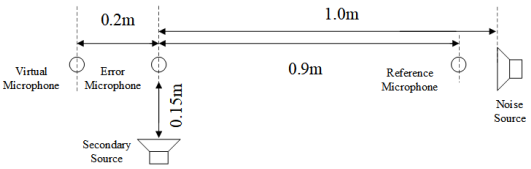

Fig. 7. Measurement arrangement.

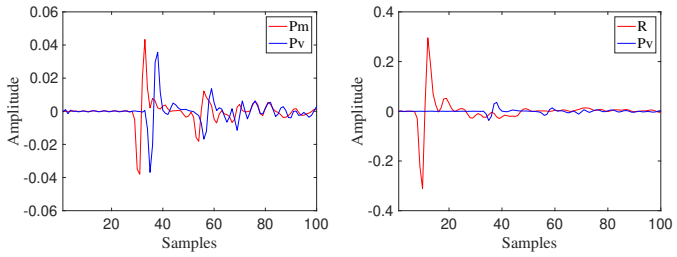

(a) P_m and P_v (b) R and P_v

Fig. 8. Impulse responses of primary paths P_m and P_v, and reference path R.

ANC system. The coherence was evaluated by MSC defined by (5) and the amount of noise reduction was evaluated by

$$\text{Reduction}(n) = 10\log_{10}\frac{\sum_{m=0}^{N-1} d_v^2(n-m)}{\sum_{m=0}^{N-1} e_v^2(n-m)}, \qquad (27)$$

where N is the tap length of the noise control filter. Simulation conditions are shown in Table I.

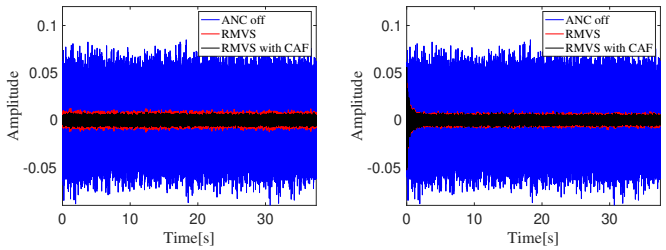

(a) $e_{d_v}(n)$ (b) $\hat{e}_v(n)$

Fig. 9. Time waveforms of error signals.

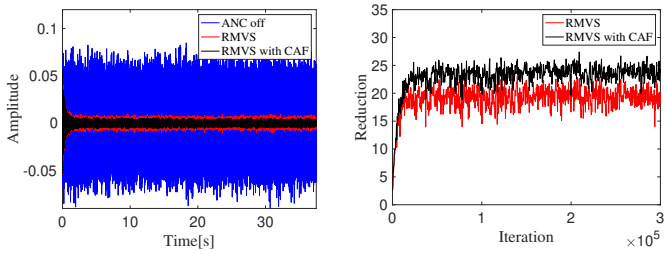

(a) Time waveform (b) Reduction

Fig. 10. Time waveforms of error signal and noise reduction at desired location and noise reduction.

In this simulation, the identified impulse responses were measured in a soundproof room shown in Fig. 6. The measurement setup is shown in Fig. 7 and the identified impulse responses of each path are shown in Fig. 8. In this identification, the reference microphone was placed at 0.9 m from the error microphone, the error microphone was placed at 0.2 m from the virtual microphone.

The paths $R(z)$, $P_m(z)$ and $P_v(z)$ are shown in Fig. 8. Delays n_d and n_r were determined by the distances between the initial peaks of $P_m(z)$ and $P_v(z)$, and $R(z)$ and $P_v(z)$, respectively. Fig. 8 shows the first 100 samples in each impulse response in order to examine the delays n_d and n_r.

To evaluate the effect of $H_1(z)$ and $H_2(z)$, we define the relative error $e_{d_v}(n)$ and error signal $\hat{e}_v(n)$ as

$$e_{d_v}(n) = \hat{d}_v(n) - d_v(n), \qquad (28)$$

$$\hat{e}_v(n) = \hat{y}'_v(n) - \hat{d}_v(n). \qquad (29)$$

The relative error $e_{d_v}(n)$ and error signal $\hat{e}_v(n)$ are shown in Fig. 9. From Fig. 9 (a), the proposed system realizes the lower relative error $e_{d_v}(n)$ than the conventional system. This means that the CAF $H_1(z)$ could make $\hat{d}_v(n)$ to be closer to the unwanted noise $d_v(n)$ than the conventional system. From Fig. 9 (b), the proposed system also realizes the lower error $\hat{e}_v(n)$ than the conventional system. This means that compare to conventional system, proposed system use the CAF $H_2(z)$ could make $\hat{y}'_v(n)$ to be closer to $\hat{d}_v(n)$.

Fig. 10 (a) compares the time waveforms of the error signal $e_v(n)$ between the proposed and conventional systems, and

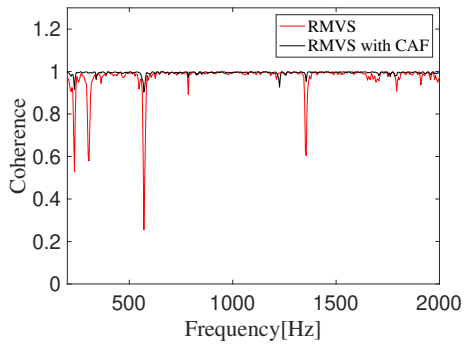

(a) Coherence of $x(n)$ and $d_v(n)$

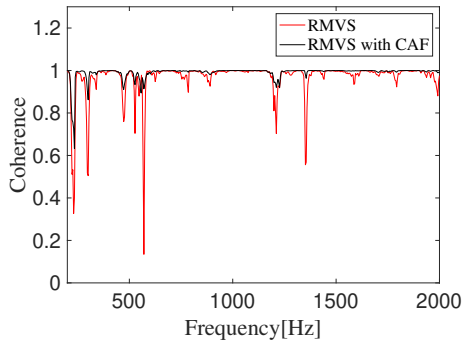

(b) Coherence of $d_m(n)$ and $d_v(n)$

Fig. 11. Magnitude-squared coherence C_{xv} and C_{mv}.

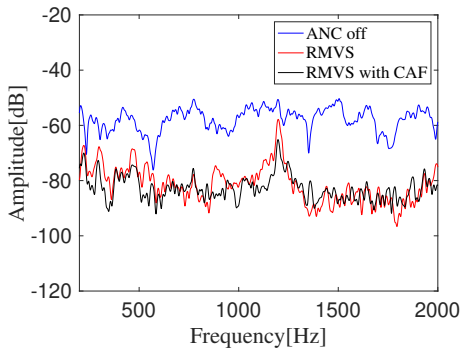

Fig. 12. Frequency spectra at the desired location.

shows that the proposed method using CAF $H_1(z)$ and $H_2(z)$ has the lower error $e_v(n)$ at desired location. From Fig. 10 (b), the proposed system can improve the amount of noise reduction by about 4 dB from the conventional feedforward ANC system with RMVS.

Fig. 11 shows the coherences $C_{xv}(w)$ and $C_{mv}(w)$ of the conventional system and proposed system. From Fig. 11, both coherences of the proposed system are higher than the conventional system. In particular, from Fig. 11 and Fig. 12, the amount of noise reduction increases at the frequency bands where the coherence is improved.

V. Conclusions

In this paper, a feedforward ANC system with RMVS and two CAFs was proposed. The conventional feedforward ANC system with RMVS degrade the noise reduction performance under low coherence condition. To improve the performance of conventional feedforward ANC system with RMVS, the proposed system uses the CAF $H_1(z)$ to adjust the noise signal $d_m(n)$ obtained at the error microphone to be close to the noise signal $d_v(n)$ obtained at the virtual microphone in the tuning stage. Furthermore, the proposed system also uses the CAF $H_2(z)$ to adjust the reference signal $x(n)$ be close to the noise signal $\hat{d}_v(n)$ in the control stage. Simulation results demonstrated that the proposed system can increase the coherences between signals obtained at reference microphone and virtual microphone, and error microphone and virtual microphone, respectively. As a result, the proposed system can improve the amount of noise reduction by about 4 dB averagely. In particular, the proposed system can improve the amount of noise reduction about 10 dB at 600 Hz and 1200 Hz where the coherence is increased. In the simulations, we only considered one measurement arrangement case. As the coherence is related to the distance of microphones, we will investigate the performance improvement of proposed system by changing the distance of reference microphone, error microphone and virtual microphone.

References

[1] S. J. Elliott, Signal Processing for Active Control, Academic Press, San Diego, CA, 2001.
[2] S. M. Kuo and D. R. Morgan, “Active noise control: a tutorial review,” Proceedings of the IEEE, vol. 87, no. 43, pp.943–973, 1999.
[3] Y. Kajikawa, W. S. Gan, and S. M. Kuo, “Recent advances on active noise control: open issues and innovative applications,” APSIPA Transactions on Signal and Information Processing, vol. 1, pp. 1–21, Aug. 2012.
[4] A. David and S. J. Elliott, “Numerical studies of actively generated quietzones,” Applied Acoustics, vol. 41, no. 1, pp. 63–79, 1994.
[5] M. Miyoshi, S. Junko, and K. Nobuo, “On arrangements of noise-controlled points for producing larger quiet zones with multi-point active noise control,” INTER-NOISE and NOISE-CON Congress and Conference Proceedings, pp. 1299–1304, 1994.
[6] Y. Kajikawa and C. Shi, “Comparison of virtual sensing techniques for broadband feedforward active noise control,” 2019 IEEE International Conference on Control, Automation and Information Sciences (ICCAIS), pp. 1–5, 2019.
[7] S. Hirose and Y. Kajikawa, “Effectiveness of headrest anc system with virtual sensing technique for factory noise,” in 2017 Asia-Pacific Signal and Information Processing Association Annual Summit and Conference (APSIPA ASC), pp. 464–468, Dec. 2017.
[8] R. Maeda, Y. Kajikawa, C. Y. Chang, S. M. Kuo, “Active Noise Control for Motor Bike Helmet Using Virtual Sensing,” 25th International Congress on Sound and Vibrations (ICSV25), pp. 1–6, 2018.
[9] S. J. Elliott and C. Jordan. “Modeling local active sound control with remote sensors in spatially random pressure fields,” The Journal of the Acoustical Society of America, vol. 137, no. 4, pp. 1936–1946, 2015.
[10] M. Moritani and Y. Kajikawa. “Improving robustness of helmet anc with auxiliary filter-based virtual sensing for head rotation,” 2021 IEEE 10th Global Conference on Consumer Electronics (GCCE), pp. 948–949, 2021.
[11] K. Iwai and T. Nishiura, “Feedforward active noise control with coherence-adjusting filter for improving noise reduction performance under low-coherence condition,” APSIPA ASC 2020, pp. 272–277, Dec. 2020.
[12] X. Kong and S. Kuo, “Study of causality constraint on feedforward active noise control systems,” IEEE Transactions on Circuits and Systems, vol. 46, no. 2, pp. 183–186, Feb. 1999.